Outer-sphere electron transfer from carbazoles to halomethanes. Reduction potentials of halomethanes measured by fluorescence quenching experiments

Sergio M. Bonesi and Rosa Erra-Balsells *

Departamento de Química Orgánica, Facultad de Ciencias Exactas y Naturales, Universidad de Buenos Aires, cc 74-suc 30, 1430, Buenos Aires, Argentina

Received (in Cambridge, UK) 17th January 2000, Accepted 26th April 2000
Published on the Web 15th June 2000

Kinetic studies on the photoinduced electron transfer reduction of a variety of halomethanes in acetonitrile and ethanol at 298 K are reported in terms of the quenching rate constants (k_q) with a series of reductants (carbazoles and anthracenes) whose one-electron oxidation potentials (E_{ox}) have been measured again in the present work *vs.* SCE and independently *vs.* ferrocene. The Rehm–Weller Gibbs energy relationship is applied to determine the fundamental parameters for the one-electron reduction, *i.e.*, the one-electron reduction potentials ($E_{RX/RX^{-\cdot}}$) of the halomethanes and the intrinsic barrier for the electron transfer reduction ($\Delta G^{\ddagger}_{o}$). The $E_{RX/RX^{-\cdot}}$ values obtained were related to the concerted electron transfer–bond breaking reduction potentials ($E_{RX/R^{\cdot}+X^{-}}$) and the standard free enthalpies of dissociation of $RX^{-\bullet}$ ($\Delta G^{o,\,diss}{}_{RX^{-\cdot}}$) were estimated in each solvent. Additionally, the one-electron reduction potential ($E_{RX/RX^{-\cdot}}$) values estimated in acetonitrile were also related to different thermodynamic parameters such as electron affinity (E_A), LUMO–HOMO energy differences (ΔE) and the bond dissociation energy (D_{RX}). Optimized geometry, E_A and ΔE for halomethanes were calculated by an *ab initio* method at the B3LYP level using 3-21G, 6-31+G(d,p) and G-311+G(3df,2pd) basis sets. In all these cases good linear correlations were obtained. The $\Delta G^{\ddagger}_{o}$ values obtained are compared with those calculated using the equation $\Delta G^{\ddagger}_{o} = \lambda/4$ with $\lambda = \lambda_i + \lambda_o$ where the solvent reorganization energy (λ_o) and the inner-sphere reorganization energies (λ_i) associated with the structural change upon the electron-transfer process were calculated, the former by using the Marcus–Hush model and the latter by using semiempirical and *ab initio* molecular modeling and QSAR properties. Results obtained from the preparative irradiation of carbazoles in the presence of halomethanes, which are consistent with a photoinduced electron transfer mechanism are also discussed.

Introduction

A major challenge in photochemistry is to find reactions of radical ions or radical ion pairs, generated through photoinduced electron transfer, which can compete with and offer a useful alternative to back-electron transfer.[1] It is known that electron transfer from the singlet radical ion pairs may occur on time scales as rapid as subnanoseconds, and any competitive process must occur on a comparable time scale unless the back-electron transfer is circumvented by techniques such as cosensitization or by enhanced and efficient cage escape.

Previous investigations of photoinduced electron transfer reactions have led to the finding of several radical ion fragmentation reactions in which relatively strong covalent bonds in the neutral (or starting molecule) rapidly cleave in the one-electron redox product. One-electron reduction of acceptors such as ethers, esters and organic halides can also result in bond cleavage.[2–7] The cleavage of the organic halides is particularly interesting since electrochemical studies as well as thermochemical calculations indicate that the carbon–halogen bond can have a negative bond energy in certain reduced halides and that the cleavage process must be extremely rapid.[5–7]

Recent investigations of the electrochemical reduction of aliphatic halides and of their homogeneous reduction by redox reagents have provided a typical example of a dissociative electron transfer process, a reaction in which the transfer of the electron and the breaking of a bond are concerted processes.[8] This particular behaviour of the alkyl halides was also observed when the photoinduced electron transfer double fragmentation reaction of aminopinacol donors[9] was studied in the presence of CCl_4 under an aerated and an inert atmosphere and also when quenching of the excited diphenylmethyl radicals by CCl_4[10] occurs. The outer-sphere heterogeneous (glassy-carbon electrodes) and homogeneous (aromatic anion radicals) reduction of the perfluoroalkyl bromides and iodides was studied by means of the dissociative electron transfer process.[11] Nevertheless, the one-electron reduction potential of CF_3I was measured using the cyclic voltammetry technique.[11] It is worth noting that Eberson[12] pointed out that i) polyhalogenated aliphatic compounds are more easily reduced than simple aliphatic halides and that ii) they might form stable anion radicals, in contrast to monohalides.[13,14]

Another feature to be taken into account in dissociative photoinduced electron transfer processes is the possibility of a termolecular back-electron transfer pathway competing effectively with the escape of fragments from the solvent cage.[15] This fact, that the fragments are formed within a solvent cage from which they may diffuse apart, and the fact that they are involved in a back-electron transfer process within the finite lifetime of the species $R^{\bullet}$ and Cl^{-} demand a more accurate method for modeling of photoinduced back-electron transfer in the dissociative electron transfer model.[16] Moreover, important experimental evidence in favor of a competitive back-electron transfer in competition with photoinduced electron transfer is the low quantum yield obtained at low conversion of the

* Correspondence address: Dra. Rosa Erra-Balsells, Departamento de Química Orgánica, FCEyN–UBA, Pabellón 2, 3º Ciudad Universitaria, 1428 Buenos Aires, Argentina. Tel/Fax: 54-11-45763346. E-mail: erra@qo.fcen.uba.ar

DOI: 10.1039/b000474j

Table 1 Irradiation of carbazole, *N*-acetylcarbazole and *N*-benzoylcarbazole in EtOH in the presence of CCl_4. Yield of photoproducts[a]

Substrate	Conv. (%)[b]	Photoproducts (%)[b] 1-chloro-carbazole	3-chloro-carbazole	3-chloro-*N*-acetylcarbazole	3-chloro-*N*-benzoylcarbazole	pH
Carbazole	15	2.0	12.5	—	—	2
N-Acetylcarbazole	12	—	—	10.3	—	2
N-Benzoylcarbazole	15	—	—	—	10.5	4

[a] Substrate concentration: 5.98×10^{-3} mol dm^{-3}; CCl_4: 5.024 mol dm^{-3}; λ_{exc}: 313 nm; irradiation time: 15 min; atmosphere: Ar; *T*: 298 K. [b] Calculated by GC.

Table 2 Irradiation of carbazole in the presence of CCl_4, in different organic solvents.[a] Yields of the photoproducts obtained

Solvent	$E_T(30)$[c]	η(cP)[d]	Photoproducts (%)[b] 1-chloro-carbazole	3-chloro-carbazole
Hexane	31.2	0.326	—	—
CCl_4	32.4	0.969	2.4	10.4
Benzene	34.5	0.652	3.2	14.2
t-BuOH	43.3	3.32	5.4	26.0
CH_3CN	46.0	0.34	4.7	25.8
i-PrOH	48.4	1.77	5.3	28.7
EtOH	51.9	1.20	4.3	30.4
MeOH	55.4	0.59	5.2	32.4

[a] Concentration of carbazole: 5.98×10^{-3} mol dm^{-3}; concentration of CCl_4: 5.024 mol dm^{-3}. [b] Calculated by GC. [c] $E_T(30)$: Reichardt values (ref. 33). [d] η(cP): viscosity of the solvent (ref. 33).

Table 4 Quantum efficiency of carbazole conversion (ϕ) in ethanol in the presence of polyhalomethanes under an inert atmosphere

Substrate	ϕ[a] CCl_4	CBr_4
2-Hydroxycarbazole	0.110	0.54
2-Methoxy-*N*-methylcarbazole	0.095	0.47
N-Methylcarbazole	0.089	0.43
Carbazole	0.068	0.41
N-Acetylcarbazole	0.066	0.37
N-Benzoylcarbazole	0.055	0.36

[a] Substrate concentration: 6.0×10^{-3} mol dm^{-3}; CCl_4: 5.0 M; CBr_4: 0.4 M; λ_{exc}: 313 nm; I_o: 1.09×10^{-6} Einstein min^{-1}; actinometer: potassium ferrioxalate.

starting material.[9] The rates of both the forward- and the back-electron transfer have been the focus of numerous investigations.[17–21] In many cases, particularly when the reactive excited state is a singlet state, the rate of the back-electron transfer is so fast that only very low efficiencies of reaction are possible unless cage escape or reaction in the solvent cage is very rapid.

Recently, we studied the photoinduced electron transfer chemical reaction of carbazole and its *N*-acyl derivatives with halomethanes in polar solvents.[22] The one-electron transfer and the carbon–halogen bond breaking processes have been proposed as steps of the reaction mechanism to explain the photoformation of the halogenated carbazoles and the strong HX acids (HCl or HBr). However, to the best of our knowledge, fundamental properties such as the one-electron reduction potentials ($E_{RX/RX^{-\cdot}}$) of the halomethanes and the intrinsic barrier for the photochemical electron transfer reactions from carbazoles to halomethanes, ($\Delta G^{\ddagger}_{o}$), are not yet available in the literature.

We report herein: (i) the results of the preparative irradiations of carbazoles in the presence of halomethanes which are consistent with a photoinduced single electron transfer mechanism (Tables 1–4) and (ii) the results of our kinetic investigations on the photoinduced electron transfer oxidation for these carbazoles and several anthracenes (see Tables 5 and 7) to determine for the first time the $E_{RX/RX^{-\cdot}}$ values of different halomethanes, which are difficult to obtain by cyclic voltammetry (Table 6). In order to do so, the one-electron oxidation potentials (E_{ox}) of carbazoles and anthracenes were measured again in the present work *vs*. SCE (Table 7) and independently *vs*. ferrocene (see Experimental). We also analyze the kinetics of the photochemical reaction in terms of the Rehm–Weller quadratic–driving force free energy relationship and we correlate the standard activation free energy ($\Delta G^{\ddagger}_{o}$) with the inner sphere reorganization energy (λ_i) as well as with the solvent reorganization energy (λ_o), both being parameters calculated in the present study; the former by using the Marcus–Hush model and the latter by semiempirical AM1, PM3 and *ab initio* methods and QSAR properties. The $E_{RX/RX^{-\cdot}}$ values obtained from the Rehm–Weller free energy relationship are related to the concerted one-electron transfer–bond-breaking reduction potential ($E_{RX/R^{\cdot}+X^{-}}$). The standard free enthalpies of dissociation of $RX^{-\bullet}$ ($\Delta G^{o,diss}{}_{RX^{-\cdot}}$) in different organic solvents are also estimated (Tables 8–13).

The one-electron reduction potential ($E_{RX/RX^{-\cdot}}$) values estimated in acetonitrile were also related to the electron affinity (E_A), the LUMO–HOMO energy difference (ΔE) and the bond dissociation energy (D_{RX}). The thermodynamic parameters

Table 3 Irradiation of the carbazole in EtOH in the presence of different polyhalomethanes (RX). Yields of the photoproducts

RX[b]	Time/h	Conversion (%)[c]	Photoproducts (%)[a] 1-chloro-carbazole	3-chloro-carbazole	1-bromo-carbazole	3-bromo-carbazole
CH_2Cl_2	30	0	—	—	—	—
$CHCl_3$	30	10.0	1.3	8.5	—	—
CCl_4	30	43.6	5.0	34.8	—	—
CH_2Br_2	30	35.0	—	—	7.0	32.0
$CHBr_3$	30	42.0	—	—	8.6	33.4
CBr_4[d]	30	47.0	—	—	7.9	37.7

[a] Calculated by GC. [b] RX: polyhalomethane, [RX]: 5.024 mol dm^{-3}. [c] Concentration of carbazole: 5.98×10^{-3} mol dm^{-3}. [d] Concentration of CBr_4: 5.98×10^{-3} mol dm^{-3}.

Table 5 Fluorescence quenching rate constants, k_q ($\times 10^{-9}$ M^{-1} s^{-1}), for excited fluorophores with different polyhalomethanes

	MeCN					EtOH		
Fluorophores	CH_2Br_2	$CHCl_3$	CCl_4	$CHBr_3$	CBr_4	CH_2Br_2	$CHCl_3$	CCl_4
2-Hydroxycarbazole	1.66	1.02	15.8	17.4	16.66	2.34	0.35	5.37
2-Methoxy-*N*-methylcarbazole	1.26	0.41	11.2	16.6	15.94	1.58	0.19	5.31
N-Vinylcarbazole	0.66	0.23	8.91	15.8	15.58	0.63	0.078	4.90
N-Methylcarbazole	0.59	0.16	6.31	14.5	16.22	0.62	0.10	4.79
N-Phenylcarbazole	0.56	0.11	—	—	—	0.49	0.036	—
2-Acetoxycarbazole	—	0.15	6.30	14.4	15.98	0.63	0.055	—
Carbazole	0.52	0.11	—	13.5	15.46	0.32	0.028	3.47
N-Acetylcarbazole	0.11	0.076	2.82	11.2	15.85	0.19	—	2.57
N-Benzoylcarbazole	0.048	0.031	1.87	9.55	—	0.11	0.017	—
3-Bromocarbazole	0.049	0.033	1.82	9.45	14.13	0.078	0.015	1.26
9-Bromoanthracene	0.016	0.0056	0.79	6.61	11.22	0.015	0.007	0.79
Anthracene	0.0089	0.0030	0.30	5.01	10.72	0.010	0.001	0.42
9,10-Dichloroanthracene	3.1×10^{-4}	0.0013	0.00631	1.26	7.59	3.3×10^{-4}	0.0015	0.062
9,10-Dibromoanthracene	1.1×10^{-4}	6.3×10^{-5}	0.0251	0.83	6.03	1.5×10^{-4}	7×10^{-5}	0.027
Anthracene-9-carboxylic acid	3.1×10^{-6}	—	0.0013	0.11	2.04	3.1×10^{-6}	—	0.0015
9-Acetylanthracene	1.6×10^{-6}	—	6.2×10^{-5}	0.019	0.65	1.8×10^{-6}	—	6.1×10^{-5}
9-Cyanoanthracene	—	—	1.0×10^{-4}	0.016	0.32	—	3.0×10^{-4}	9.5×10^{-5}

Table 6 Thermodynamic parameters of the polyhalomethanes[a]

Polyhalomethanes	E_{red}[b]/V *vs.* SCE	E_A[c]/eV	E^{HOMO}[d]/eV	E^{LUMO}[d]/eV	ΔE[e]/eV	D_{RX}[f]/eV
CH_2Cl_2		0.201	−10.903	8.261	19.159	3.63[g]
$CHCl_3$	−1.90	0.320	−11.551	6.807	18.354	3.51
CCl_4	−1.68	0.486	−11.878	5.297	17.175	3.17
CH_2Br_2	−1.84	0.503	−9.083	8.045	17.128	3.08
$CHBr_3$	−1.55	0.624	−8.785	6.751	15.536	3.03
CBr_4	−1.38	0.820	−9.017	5.585	14.602	2.44
CF_3Br	−1.48[h]	0.806[i]	−13.751	8.082	21.833	3.08
CF_3I	−1.22[h]	1.203[i,j]	−9.839[k]	5.953[k]	15.752[k]	2.01

[a] Calculations were performed at the B3LYP/6-311+G (3df,2pd) level for optimized geometries and at the B3LYP/6-31+G(d,p) level for frequency calculations and thermodynamic parameters at 298 K; for CF_3I the 3-21G basis set was used at the B3LYP level. [b] Values determined in this work. [c] Values calculated according to eqn. (7) at the B3LYP/6-31+G(d,p)//B3LYP/6-311+G(3df,2pd) level. [d] Values calculated at the ZINDO-1//B3LYP/6-311+G(3df,2dp) level. [e] Values calculated according to eqn. (8) at the ZINDO-1//B3LYP/6-311+G(3df,2dp) level. [f] Data from ref. 45(*b*). [g] Data from ref. 45(*c*). [h] Values calculated in this work by using the Rehm–Weller model and taking the rate constant values (k_1) from ref. 11. [i] E_A values reported in ref. 45(*d*): CF_3Br, 0.91 ± 0.2; CF_3I, 1.57 ± 0.2 eV. [j] Values calculated at the B3LYP/3-21G//B3LYP/3-21G level. [k] Values calculated at the ZINDO-1//B3LYP/3-21G level.

Table 7 Properties of the fluorophores used in this study

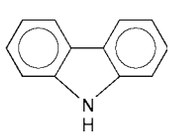

Carbazoles

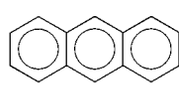

Anthracenes

	MeCN				EtOH			
Fluorophores	τ/ns	E_{ox}/ V *vs.* SCE	E_{oo}/eV	E^*_{ox}/ V *vs.* SCE	τ/ns	E_{ox}/ V *vs.* SCE	E_{oo}/eV	E^*_{ox}/ V *vs.* SCE
2-Hydroxycarbazole	12.46	0.87	3.80	−2.93	12.26	0.90	3.78	−2.88
2-Methoxy-*N*-methylcarbazole	14.69	0.90	3.64	−2.74	14.31	0.95	3.67	−2.72
N-Vinylcarbazole	11.14	0.94	3.57	−2.63	9.61	0.96	3.62	−2.66
N-Methylcarbazole	14.72	1.03	3.54	−2.51	13.92	0.99	3.56	−2.57
N-Phenylcarbazole	11.35	1.08	3.60	−2.52	10.92	1.09	3.58	−2.49
2-Acetoxycarbazole	13.19	1.21	3.68	−2.47	—	—	—	—
Carbazole	15.13	1.10	3.59	−2.49	14.44	1.14	3.55	−2.41
N-Acetylcarbazole	13.20	1.62	3.91	−2.29	12.40	1.52	3.86	−2.30
N-Benzoylcarbazole	10.20	1.55	3.78	−2.23	—	—	—	—
3-Bromocarbazole	13.18	1.20	3.54	−2.34	13.03	1.17	3.50	−2.09
9-Bromoanthracene	1.05	1.20	3.35	−2.15	—	—	—	—
Anthracene	5.30	1.15	3.31	−2.12	5.30	1.25	3.27	−2.02
9,10-Dichloroanthracene	2.10	1.26	3.19	−1.93	2.00	1.25	3.21	−1.96
9,10-Dibromoanthracene	1.80	1.28	3.17	−1.89	1.90	1.29	3.19	−1.90
Anthracene-9-carboxylic acid	4.10	1.43	3.12	−1.69	4.20	1.42	3.10	−1.68
9-Acetylanthracene	4.70	1.38	3.00	−1.61	4.50	1.38	3.00	−1.62
9-Cyanoanthracene	12.4	1.53	3.10	−1.57	>5	1.53	3.07	−1.54

Table 8 Parameters for Rehm–Weller fits of fluorescence quenching data

Polyhalomethanes	MeCN			EtOH		
	E_{red}[a]/ V *vs.* SCE	λ[b]/eV	$k_{max}k_{diff}$/ 10^{10} M^{-1} s^{-1}	E_{red}[a]/ V *vs.* SCE	λ[b]/eV	$k_{max}k_{diff}$/ 10^{10} M^{-1} s^{-1}
CH_2Br_2	−1.83	1.50	20	−1.88	1.33	12.1
$CHCl_3$	−1.90	1.44	10	−1.98	1.55	10.1
CCl_4	−1.68	1.43	100	−1.70	1.33	61.7
$CHBr_3$	−1.55	1.20	111.1			
CBr_4	−1.46	0.98	87			

[a] ±0.08 V. [b] ±0.15 eV.

Table 9 $\Delta G^{\ddagger}_o$ values of the photoinduced reduction of the polyhalomethanes in acetonitrile and in ethanol

RX	MeCN			EtOH		
	$\Delta G^{\ddagger}_o$(exp)[a]	$\Delta G^{\ddagger}_o$(theo)[b]	$\Delta G^{\ddagger}_o$(prtd)[c]	$\Delta G^{\ddagger}_o$(exp)[a]	$\Delta G^{\ddagger}_o$(theo)[b]	$\Delta G^{\ddagger}_o$(prtd)[c]
CH_2Br_2	0.38	0.38	1.15	0.33	0.38	1.16
$CHCl_3$	0.36	0.35	1.23	0.39	0.34	1.24
CCl_4	0.36	0.31	1.10	0.33	0.33	1.11
$CHBr_3$	0.30	0.33	1.10	—	—	—
CBr_4	0.25	0.33	0.94	—	—	—
Average value	0.33	0.34	1.09	0.35	0.35	1.17

[a] Values determined in this work. [b] Values calculated according to: $\Delta G^{\ddagger}_o = (\lambda_o + \lambda_i^D + \lambda_i^A)/4$. [c] Values calculated according to eqn. (9).

Table 10 Reorganization energies (λ_i) of the carbazole radical cations and of polyhalomethane radical anions and their hard-sphere radii calculated by computational molecular modelling methods

Carbazoles	λ_i^D/eV[a]	r_D/Å[b]	Polyhalomethanes	λ_i^A/eV	r_A/Å[c]
Carbazoles	0.31	5.07	CH_2Br_2	0.45	4.1
N-Methylcarbazole	0.30	5.21	$CHCl_3$	0.29	4.1
N-Phenylcarbazole	0.11	5.61	CCl_4	0.16	4.3
N-Vinylcarbazole	0.03	5.29	$CHBr_3$	0.23	4.3
N-Acetylcarbazole	0.14	5.30	CBr_4	0.17	4.6
N-Benzoylcarbazole	0.24	5.57			
2-Hydroxycarbazole	0.32	5.13			
2-Acetoxycarbazole	0.33	5.44			
3-Bromocarbazole	0.29	5.26			
2-Methoxy-*N*-methylcarbazole	0.32	5.30			
Anthracene	0.13	5.18			
9-Bromoanthracene	0.13	5.32			
9,10-Dibromoanthracene	0.19	5.45			
9-Cyanoanthracene	0.32	5.32			
9-Anthranylcarbonitrilic acid	0.12	5.34			
9-Acetylanthracene	0.13	5.29			
9,10-Dichloroanthracene	0.17	5.36			

[a] The λ_i^D average value is 0.22 eV. [b] The r_D average value is 5.32 Å (calculated by the QSAR method). [c] The r_A average value is 4.3 Å (calculated by the QSAR method).

Table 11 Experimental and theoretical parameters of the reduction of the polyhalomethanes

Polyhalomethanes	MeCN (λ_o = 0.86 eV[a])		EtOH (λ_o = 0.82 eV[a])	
	λ_{exp}/eV	λ_{calcd}[b]/eV	λ_{exp}/eV	λ_{calcd}[b]/eV
CH_2Br_2	1.50	1.53	1.33	1.57
$CHCl_3$	1.44	1.41	1.55	1.45
CCl_4	1.43	1.24	1.33	1.28
$CHBr_3$	1.20	1.31	—	—
CBr_4	0.98	1.32	—	—
Average value	1.31	1.35	1.40	1.39

[a] Calculated from eqn. (8). [b] Rough estimation (see text). The λ_i^D value is 0.22 eV and was taken as an average value from Table 8.

Table 12 Estimated $E_{RX/R^{\cdot} + X^-}$ values in acetonitrile and ethanol

Polyhalomethanes	$E_{RX/R^{\cdot} + X^-}$[a]			
	MeCN		EtOH[b]	
	$\Delta G_{RX/R^{\cdot}} = 0$	$\Delta G_{RX/R^{\cdot}} \neq 0$	$\Delta G_{RX/R^{\cdot}} = 0$	$\Delta G_{RX/R^{\cdot}} \neq 0$
CH_2Br_2	−1.43	−1.31	−1.10	−0.98
$CHCl_3$	−1.58	−1.47	−1.15	−1.04
CCl_4	−1.12	−1.01	−0.69	−0.58
$CHBr_3$	−1.38	−1.26	—	—
CBr_4	−0.86	−0.74	—	—

[a] All potentials are given *vs.* SCE. [b] The ΔE^o(SHE→SCE) value in ethanol was taken to be equal to that in acetonitrile, −0.255 V.

Table 13 Free enthalpy of dissociation ($\Delta G^{o,diss}(RX^{-\bullet})$) values of the polyhalomethane anion radical in acetonitrile and ethanol

Polyhalomethanes	$\Delta G^{o,diss}(RX^{-\bullet})$[a]			
	MeCN		EtOH	
	$\Delta G_{RX/R^{\cdot}} = 0$	$\Delta G_{RX/R^{\cdot}} \neq 0$	$\Delta G_{RX/R^{\cdot}} = 0$	$\Delta G_{RX/R^{\cdot}} \neq 0$
CH_2Br_2	−0.40	−0.52	−0.78	−0.90
$CHCl_3$	−0.12	−0.23	−0.83	−0.94
CCl_4	−0.48	−0.59	−1.01	1.12
$CHBr_3$	−0.17	−0.29	—	—
CBr_4	−0.60	−0.72	—	—

[a] All the energy values are given in eV.

E_A and ΔE, and the optimized geometries were calculated in the present study combining *ab initio* and semiempirical methods at the B3LYP//B3LYP and ZINDO-1//B3LYP levels, using different basis sets (3-21G; 6-31+G(d,p) and 6-311+G(3df,2pd)) (Table 6). In all these cases good linear correlations have been observed.

Experimental

Materials

N-Acetylcarbazole,[23] *N*-benzoylcarbazole,[24] 3-bromocarbazole,[25] 2-acetoxycarbazole and 2-methoxy-*N*-methylcarbazole[26] were prepared according to the procedures that we have described previously. *N*-Phenylcarbazole, *N*-methylcarbazole, *N*-vinylcarbazole, 2-hydroxycarbazole and carbazole were purchased from Aldrich and were used without further purification.

Spectrograde chloroform, tetrachloromethane, methylene bromide and tribromomethane were obtained from Aldrich and were used as received. Acetonitrile and ethanol used as solvents were purified and dried by standard procedure.[27]

Anthracene, 9-bromoanthracene, 9,10-dibromoanthracene, 9,10-dichloroanthracene, 9-acetylanthracene and anthracene-9-carboxylic acid were obtained from Aldrich and were recrystallized from ethanol before use. 9-Cyanoanthracene was purchased from Kodak and was used as received.

Photoirradiations

General procedure: Solutions of carbazole (6.0 mmol) and CCl_4 (50 mmol) were prepared in different organic media (10 mL). A 2 mL aliquot of the solution was placed in a 3 mL quartz stoppered cell and was bubbled with dry Ar (or N_2) for 20 minutes. The cell was placed on an optical bench and was irradiated with a high pressure Hg lamp (450 W, Ealing Co.) whose radiation was collimated (quartz lens) and filtered with an interference filter (Schott, path band: 5 mm) to give a nearly parallel beam at 313 nm. The progress of the reaction was monitored by TLC and GC analysis (Ultra-2 capillary column). The products obtained in the photolyzed solution were identified by comparison of their R_t (retention time in GC) and MS (GC-MS technique) values with those of the authentic samples prepared by thermal synthesis previously described (chlorocarbazole derivatives of carbazole and 2-hydroxycarbazole see ref. 25; chlorocarbazole derivatives of *N*-methylcarbazole, 2-methoxy-*N*-methylcarbazole, *N*-acetylcarbazole and *N*-benzoylcarbazole, see ref. 26). The photoproduct chemical yields and the conversion of the starting material in the photolyzed solution were determined by quantitative GC using internal standards.

The irradiations were also carried out in the presence of different polyhalomethanes (CH_2Cl_2, $CHCl_3$, CH_2Br_2, $CHBr_3$ and CBr_4; 50 mmol) according to the general procedure described above.

Quantum yield

Quantum yields were determined using potassium ferrioxalate as an actinometer.[28] A 6×10^{-3} mol dm^{-3} solution of $K_3Fe(C_2O_4)_3 \cdot 3H_2O$ was prepared for measurements done on an optical bench at 313 nm. Simultaneously, the carbazole solutions, prepared according to the general procedure, were irradiated in the same optical set. The conversion of carbazoles and the formation of the photoproducts were monitored by GC.

Luminescence quenching

Fluorescence lifetime values (τ) were measured using an Edinburgh OB900 fluorometer. UV absorption spectra were recorded using a Hewlett Packard HP 8541 A UV-visible diode array spectrophotometer. Fluorescence measurements were performed on a Perkin-Elmer LS5 spectrofluorimeter whose output is automatically connected for instrumental response by means of a Rhodamine B quantum counter and equipped with a Hamamatsu R928 photomultiplier tube. The excitation spectra were performed on the same spectrometer. The fluorescence emission and excitation spectra of the solvent blanks were run in each case, to check that they showed negligible emission over the wavelength range monitored for emission and excitation experiments. The measurements at room temperature (298 K) were recorded with stoppered quartz cells of 1 cm using 90° mode.

The excitation wavelength used for 2-methoxy-*N*-methylcarbazole, 2-acetoxycarbazole and 2-hydroxycarbazole was 320 nm and for 3-bromocarbazole was 343 nm, while for the other carbazole derivatives the excitation wavelength was 310 nm. The monitoring wavelengths were those corresponding to the maxima of the respective emission bands ranging from 355 to 375 nm.

Relative emission intensities were measured for acetonitrile and ethanol solutions containing the fluorophores (5×10^{-5} mol dm^{-3}) together with a halomethane quencher at various concentrations (1×10^{-4}–2×10^{-2} mol dm^{-3}). The Stern–Volmer relationship was used to obtain the quenching rate constant values (k_q) from the slopes of the linear correlation between the ratio τ_o/τ and the concentration of the quencher (halomethanes). All the measurements were performed under degassed conditions (Ar or N_2).

Cyclic voltammetry

The cyclic voltammetry measurements were performed on a Pine Bipotentiostat AFRDE5 potentiostat-galvanostat in deaerated MeCN and in EtOH containing 1.0×10^{-1} mol dm^{-3} Et_4NClO_4 as a supporting electrolyte at 298 K. The measured potentials were recorded with respect to the saturated calomel electrode (SCE). Also, the measured potentials were checked by adding to the analyte solution 0.25 mL of 1.0×10^{-1} mol dm^{-3} ferrocene in order to report accurate one-electron oxidation potentials of carbazoles. The platinum microelectrode was routinely cleaned by soaking it in a concentrated sulfuric acid–nitric acid mixture (1 : 1; v/v), followed by repeated rinsing with water and acetone and drying at 353 K prior to use in order to avoid possible fouling of the electrode surface. The counter electrode (CE) was platinum and the cyclic voltammograms were recorded at a sweep rate of 100 mV s^{-1}.

Theoretical calculations

For halomethanes all geometries were fully optimized without imposing any symmetry constraints. For our density functional theory (DFT) calculations, we used the hybrid gradient-corrected exchange functional proposed by Becke,[29c,e] combined with the gradient-corrected correlation functional of Lee, Yang, and Parr.[29d] This functional is commonly known as B3LYP and has been shown to be quite reliable for geometries. For geometry optimizations the standardized 6-311G basis set

was used together with diffuse functions (+) and with polarization functions (d,f,p). We denote our B3LYP calculations by B3LYP/6-311+G(3df, 2pd). For frequency calculations the standardized 6-31+G(d,p) basis set was used at the B3LYP level. For CF_3I, calculations were performed with the B3LYP/3-21G//B3LYP/3-21G method. The (LUMO–HOMO) values were calculated with the ZINDO-1//B3LYP/6-311+G(3df, 2pd) method, and for CF_3I with the ZINDO-1//B3LYP/3-21G method. The ground-state geometry and heat of formation of carbazoles and anthracenes were calculated by using the semiempirical parametrized AM1 and PM3 methods as implemented in a version of the HyperChem Suite program.[29a] PM3 has proved to be effective in studies on molecules containing heteroatoms, compared with other methods such as MINDO/3 or MNDO.[29a,b] The geometries of the radical ions were optimized using an unrestricted Hartree–Fock (UHF) formalism. The reorganization energies of the inner coordination spheres (λ_i) associated with the structural change of the substrate upon electron transfer were calculated as the difference in ΔH_f of the radical ions with the same structures as the neutral forms and ΔH_f with the optimized structures using the UHF formalism. All the *ab initio* calculations were carried out using the Gaussian 98W program.[30b]

Results

I. Preparative irradiations

In previous work we demonstrated that carbazole derivatives in the excited state photosensitize the decomposition of CCl_4, working as electron donors.[22] The carbazoles employed were *N*-acetyl- and *N*-benzoylcarbazole. Laser flash photolysis experiments confirmed the intermediacy of donor cation radical species and the characterization of the photoproducts in the photolyzed solution showed that the carbon–halogen bond of CCl_4 cleaved during irradiation. Despite this earlier work it seemed worthwhile to study in detail the photochemical behaviour of other carbazoles in the presence of CCl_4. Thus, when ethanolic solutions of carbazole were irradiated in the presence of CCl_4 (5.02 mol dm^{-3}) under an argon atmosphere, the formation of chlorocarbazole derivatives (1-chloro- and 3-chlorocarbazole) was observed at low conversion of carbazole (15%) (Table 1). Also in the photolyzed solution, hexachloroethane (C_2Cl_6) was detected (GC-MS) as well as $HCCl_3$ (GC-MS) and HCl. The photochemical reaction is depicted in Scheme 1.

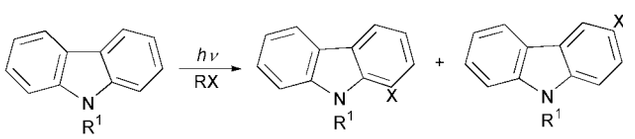

R^1	RX	X
H; CH_3CO; PhCO	$CHCl_3$; CCl_4	Cl
H; CH_3CO; PhCO	CH_2Br_2; $CHBr_3$; CBr_4	Br

Scheme 1

The effect of the properties of the solvents on the photochemical reaction between carbazole and CCl_4 was studied in hexane, CCl_4, benzene, *tert*-butyl alcohol, isopropanol, methanol, ethanol and acetonitrile. Thus, the irradiation of carbazole in the presence of CCl_4 was carried out in the above mentioned organic media under a nitrogen atmosphere, and chlorocarbazole derivatives were obtained as photoproducts (Table 2). From these results it was concluded that an increase in the polarity of the solvent expressed as $E_T(30)$ (Reichardt parameter) produces a slight increase in the yield of the chlorocarbazole derivatives while no effect was observed on the photochemical reaction when polar aprotic or polar protic solvents were used. Also, the slight effect of the solvent polarity on the photochemical reaction would account for the formation of species of higher polar character than the substrates such as a polar exciplex $[D^{\delta+} \cdots RX^{\delta-}]$ formed after the excitation of the electron donor (D*).

The influence of the electron affinity of the halomethanes such as CH_2Cl_2, $CHCl_3$, CCl_4, CH_2Br_2, $CHBr_3$ and CBr_4 on the photochemical reaction of carbazole was also analyzed. The irradiations were carried out in ethanol under a nitrogen atmosphere and the monochloro- and monobromocarbazoles were obtained as photoproducts. The conversion of carbazole and the yields of the photoproducts obtained are presented in Table 3. As is shown in the Table, the conversion of carbazole at a given irradiation time increases significantly as the electron affinity of the polyhalomethane increases. When CH_2Cl_2 was the halomethane used, carbazole was recovered unchanged. The lower electron affinity of CH_2Cl_2 would account for this result. Similar results were obtained when *N*-acetylcarbazole, *N*-benzoylcarbazole, *N*-methylcarbazole, 2-hydroxycarbazole and 2-methoxy-*N*-methylcarbazole were irradiated in the presence of CCl_4 or CBr_4 in acetonitrile or in ethanol solution; the corresponding monochlorocarbazole and monobromocarbazole derivatives were obtained as photoproducts. In summary, the quantum efficiencies of carbazole conversion in ethanol, in the presence of CCl_4 and CBr_4 are shown in Table 4.

II. Fluorescence quenching studies

Simultaneously we studied in detail the fluorescence quenching of the above mentioned carbazoles (fluorophores) using CH_2Cl_2, $CHCl_3$, CCl_4, CH_2Br_2, $CHBr_3$ and CBr_4 as quenchers.

The fluorescence quenching experiments were carried out measuring the half lifetime of the carbazole singlet excited state (τ and τ_o) by using the time correlated–single photon counting (TC–SPC) technique. The τ values measured at various quencher concentrations were fitted to the Stern–Volmer relationship (eqn. (1)).

$$\tau_o/\tau = 1 + k_q\tau_o[Q] \quad (1)$$

It is interesting to note that the halogenated compounds quench the fluorescence emission of the carbazoles and no new emission bands are observed when a stationary fluorescence quenching technique is used.

The rate constants for fluorescence quenching, k_q, were determined from measured $k_q\tau_o$ and carbazole and anthracene τ_o values. The k_q values obtained are listed in Table 5. As can be seen in the table the quenching rate constant is higher when the electron affinity (E_A) of the quencher is higher (Table 6) and when the E^*_{ox} of the fluorophore becomes lower (Table 7). Also, it is observed that the limit k_q values (diffusional rate constant, k_{diff}, limit value[31] 1.9×10^{10} M^{-1} s^{-1} and 6.79×10^9 M^{-1} s^{-1} in acetonitrile and ethanol, respectively) are reached when E^*_{ox} reaches the lowest value (less than -3.0 V (*vs.* SCE)). The k_q values were also correlated to the singlet energy, E_{oo}, of the carbazoles (Table 7).

III. Redox properties

The efficiency and ability of the carbazoles to yield the reduction of the halogenated compounds are qualitatively related to their excited state oxidation potentials, E^*_{ox}, which are listed in Table 7.[32] These E^*_{ox} values were calculated according to eqn. (2), where the oxidation potentials (E_{ox}) were

$$E^*_{ox} = E_{ox} - E_{oo} \quad (2)$$

measured by cyclic voltammetry (see Experimental), while the singlet state energies, E_{oo}, were determined by superimposing

the fluorescence excitation spectra and the fluorescence emission spectra, both normalized and run in acetonitrile and in ethanol. E_{ox} is in volts (*vs.* SCE) and E_{oo} is in eV.

We have also calculated the E^*_{ox} values of some anthracene derivatives according to eqn. (1) in order to enlarge the E^*_{ox} range of the $\log(k_q) - E^*_{ox}$ correlations and to improve the fit of our experimental data by application of the Rehm–Weller energy relationship (see Discussion). These E^*_{ox} values are listed in Table 7 together with those of carbazoles, and the corresponding k_q values measured in quenching experiments are shown in Table 5. Thus, a wide range of E^*_{ox} was obtained (−1.5 to −3.0 V *vs.* SCE) for the application of the Rehm–Weller energy relationship. Although some data have been previously reported,[33] the one-electron oxidation potentials, E^*_{ox}, of carbazole and anthracene derivatives were measured again in the present work, in acetonitrile and in absolute ethanol, in the presence of tetraethylammonium perchlorate under a nitrogen atmosphere at 298 K. The saturated calomel electrode was chosen as the reference electrode. Also, a solution of ferrocene (5.00×10^{-2} mol dm^{-3}) was added to the analyte solutions in order to check the accuracy of the E^*_{ox} obtained; the values obtained are listed in Table 7.

Discussion

The photochemical decomposition of polyhalomethanes such as $CHCl_3$, CCl_4, CH_2Br_2, $CHBr_3$ and CBr_4, by carbazoles has been shown to be an efficient process which gives halocarbazole derivatives as photoproducts with good chemical yields. As is shown in Table 2 the observed slight solvent effect on the photochemical reaction suggests the formation of intermediate reaction species of higher polar character than the substrates such as polar to ionic species. Simultaneously, the viscosity effect on the photoproduct distribution (chlorocarbazole derivatives) accounts for the fact that these photoproducts would be formed in the solvent cage. Both results together suggest the formation in the solvent cage of polar intermediate species as a consequence of the interactions of the carbazole in the singlet excited state and the polyhalomethane. As is shown in Tables 1 and 3 the photochemical reaction occurs efficiently with the yields being dependent on the redox properties of the carbazole and the polyhalomethane; thus, for a fixed polyhalomethane, *i.e.* CCl_4, the quantum yield of conversion of the carbazoles increases significantly as the excited oxidation potential of the carbazoles (E^*_{ox}) becomes more negative (Table 7). In the same way, at a fixed fluorophore, *i.e.*, carbazole, the conversion shows a noticeable increase when the electron affinity (E_A) of the halomethane is higher and the ΔE(LUMO–HOMO) value of the halomethane is lower (Table 6). The results given above, together with the fact that for *N*-acylcarbazoles irradiated in the presence of CCl_4 the corresponding cation radical species could be characterized, agree with a reaction mechanism which involves a single electron transfer from the excited carbazole (donor) to the polyhalomethane (acceptor).

Connected with this, and in order to understand better the photochemical reaction mechanism, fluorescence quenching experiments were carried out simultaneously with the photopreparative studies. As can be seen in Table 5, the k_q values measured increase as the E^*_{ox} of the fluorophores (carbazoles) become more negative, reaching the diffusional rate constant limit value (k_{diff}) when the E^*_{ox} value is less than −3.0 V (*vs.* SCE) (Table 7). Also, in the same table it is shown that the k_q values increase as the electron affinity of the halomethanes increases (Table 6). The observed correlation of the k_q values with the carbazole E^*_{ox} values and with the halomethane E_A values as well as with the halomethane ΔE(LUMO − HOMO) values (see Table 6) agrees with the photoinduced single-electron transfer mechanism proposed for the photochemical yield of chlorocarbazoles.

It is worth noting that the correlations of the carbazole conversion and the chemical yield of chlorocarbazole derivatives (Tables 1, 3 and 4) with both the carbazole E^*_{ox} (Table 7) and the halomethane E_A (Table 6) show similar trends to those observed for the k_q values.

In summary, this photochemical process can be represented as a photochemical reaction initiated by a photoinduced single-electron transfer from carbazole, in its singlet electronic excited state, to the polyhalomethane, initially forming a contact pair. The contact pair yields, after the electron transfer process, a radical ion pair in the solvent cage. In the same solvent cage the necessary steps to generate the chlorocarbazole derivatives should also occur.[22,24b,34,35]

Generally speaking, photochemical electron transfer reactions occur only when the charge transfer step is either exergonic or slightly endergonic (< 0.22 eV).[36,37] In these cases charge transfer is fast enough to compete with non-radiative (radiationless) deactivation of the excited singlet state of the fluorophore. In order to determine the extent of the thermodynamic feasibility of the photochemical reaction, the E_{red} ($RX/RX^{-\cdot}$) value of the halomethane needs to be known or estimated.

Nevertheless, very little is known about the one-electron reduction potentials ($E_{red}(RX/RX^{-\cdot})$) of the polyhalomethanes (RX) and a key consideration in evaluating any proposed photochemical single-electron transfer mechanism is the free energy change in the charge transfer step (first step in Scheme 2).

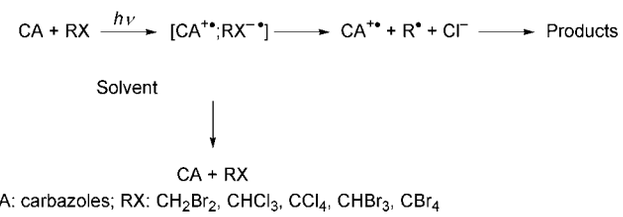

Scheme 2 Mechanism for the photochemical reaction of carbazoles.

The estimation of the one-electron reduction potential of the polyhalomethanes can be done from a quantitative point of view by analyzing the correlation between the k_q values and the E^*_{ox} of the electron donors by using the Rehm–Weller model.[36] Thus, the fluorescence quenching process was also analyzed from the quantitative point of view by using the above mentioned model.[36] According to this model the process can be divided into four steps as is shown in Scheme 3.[34]

$$S^* + Q \underset{k_{-diff}}{\overset{k_{diff}}{\rightleftharpoons}} [S;Q]^*$$
(encounter complex)
$$[S;Q]^* \underset{k_{-et}}{\overset{k_{et}}{\rightleftharpoons}} [S^{+\cdot};Q^{-\cdot}] \xrightarrow{k_{bet}} S + Q$$
(contact ion pair)
$$[S^{+\cdot};Q^{-\cdot}] \xrightarrow{k_3} \text{Products}$$

Scheme 3 Reaction mechanism.

There is an initial diffusive encounter (k_{diff}) of the excited state donor molecule (S*) with the ground state quencher molecule Q forming an encounter complex ([S;Q]*). The latter undergoes a charge transfer (k_{et}) to form a contact ion-pair (also known as a successor complex). The contact ion-pair decays through a number of pathways including, among others: solvent relaxation; C–X bond dissociation (where X is a halogen); free ions escaping out of the solvent cage to yield products, which are grouped under the rate constant k_3, back-electron transfer (k_{bet}) leading to ground state reactants, S and Q, and k_{-et} reversing to the encounter complex.

The quenching rate constant (k_q) is the overall rate constant for the loss of S* due to reaction with Q. On application of the

steady-state approximation to the encounter complex and the contact ion pair, both shown in Scheme 3, with the further assumption[38] that $k_3 \gg k_{-et}$ and substituting k_{et} with the Eyring expression ($k_{et} = k_{max}\exp(-\Delta G^{\ddagger}/RT)$), eqn. (3) was obtained.

$$k_q = k_{diff}/[1 + k_{diff}/K_{diff}k_{max}\exp(-\Delta G^{\ddagger}/RT)] \quad (3)$$

K_{diff} is known as the diffusional equilibrium constant and k_{max} is the so-called frequency factor.

The free energy barrier for the electron transfer step, $\Delta G^{\ddagger}$, can be predicted from the driving force of the electron transfer reaction, ΔG°, along with the reorganization energy λ. There are a number of treatments of this relationship,[37] the most widely used in fluorescence quenching data is the Rehm–Weller energy relationship.[36] Eqn. (4) shows the monotonic relationship between $\Delta G^{\ddagger}$ and ΔG°, where ΔG° is the free energy change of the electron transfer step. All the free energy values are in eV.

$$\Delta G^{\ddagger} = \Delta G^{\circ}/2 + [(\Delta G^{\circ}/2)^2 + (\lambda/4)^2]^{1/2} \quad (4)$$

On the other hand, the ΔG° values for the photoinduced electron transfer process are obtained according to the eqn. (5),

$$\Delta G^{\circ} = E^*_{ox} - E_{red} - E_{coul} \quad (5)$$

where E^*_{ox} is the one-electron potential oxidation of the donor in its singlet excited state (calculated from eqn. (2)), E_{red} is the one-electron potential reduction of the acceptor in its ground state and E_{coul} is the term that accounts for desolvation and Coulombic interactions in the ion pair as described by $q/\varepsilon r$. The values of E^*_{ox} and the experimentally derived k_q values shown in Tables 5 and 7, were analyzed using eqns. (3)–(5). The two adjustable parameters were λ and E_{red}.

As is shown in Table 5 we have also included the experimental k_q values obtained in fluorescence quenching experiments with anthracene, 9-bromoanthracene, 9,10-dibromoanthracene, 9,10-dichloroanthracene, 9-acetylanthracene, anthracene-9-carboxylic acid and 9-cyanoanthracene and the five halomethanes used in the present work. We have selected these anthracene derivatives because their spectroscopic properties are similar to those of the carbazole derivatives and also because their one-electron reduction capabilities toward the halomethanes are lower than those of carbazoles. It is also important to mention that the radical cations of the anthracene derivatives show a hard-sphere radius (r_D) and a reorganization energy (λ_i^D) quite similar to those of carbazoles (see Table 10). The inclusion in our study of these anthracene derivatives has allowed us to enlarge the E^*_{ox} range of the $\log(k_q) - E^*_{ox}$ plots obtained (see later, Figs. 1–3) and, as a consequence to improve the fit of our experimental data by application of the Rehm–Weller energy relationship.

It is worth noting that the first parametrization was carried out by taking the originally estimated value for the preexponential term, $k_{max}K_{diff}$, to be 10^{11} M^{-1} s^{-1}.[36] Nevertheless, the appropriate value of this term has been the subject of some recent discussion. It has been shown that certain fluorescence data can be made to conform to the Marcus theory by revising this factor upward.[39–41] Marcus[42] and Weaver[43] have analyzed the k_{max} factor and have argued that in acetonitrile it should take a value of 10^{12} to 10^{13} s^{-1}. The other factor of the preexponential term, K_{diff}, has not been subjected to the same level of analysis. Of course, we do not attempt to establish the optimal value of each of the two factors of the preexponential term because the measurements reported here are sensitive only to the product of these two parameters and are unable to resolve the individual contributions.

Taking into account the above consideration, the value for $k_{max}K_{diff}$ was not fixed. Instead, 10 to 20 fits were undertaken for each donor as this parameter was systematically varied from 10^{10} to 10^{14} M^{-1} s^{-1}. We observed that while the quality of the fits varied significantly over the range, the E_{red} values were relatively insensitive to large changes in $k_{max}K_{diff}$. The best fit values of $k_{max}K_{diff}$ found are listed in Table 8.

The reduction potential of the halogenated compounds (E_{red}) and λ values were estimated from the experimental determined k_q values and the calculated E^*_{ox} values by using a simplex algorithm where the sums of the squares of the residuals are minimised as the parameters λ and E_{red} are varied. The optimised plots along with the experimental data are presented in Figs. 1–3. Table 8 lists the best fit values of λ and E_{red}.

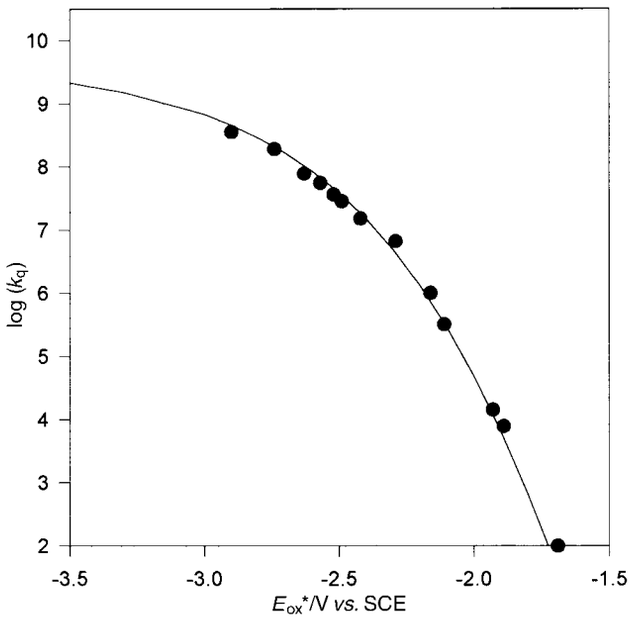

Fig. 1 Rehm–Weller analysis of the dependence of the fluorescence quenching rate constant (k_q in M^{-1} s^{-1}) for $CHCl_3$ (filled circles) on the excited state oxidation potentials (E_{ox}* in V *vs.* SCE) of various sensitizers (carbazoles and anthracenes, see Tables 5 and 7) in MeCN. Curve (solid line) shows the fit calculated according to the Rehm–Weller model.

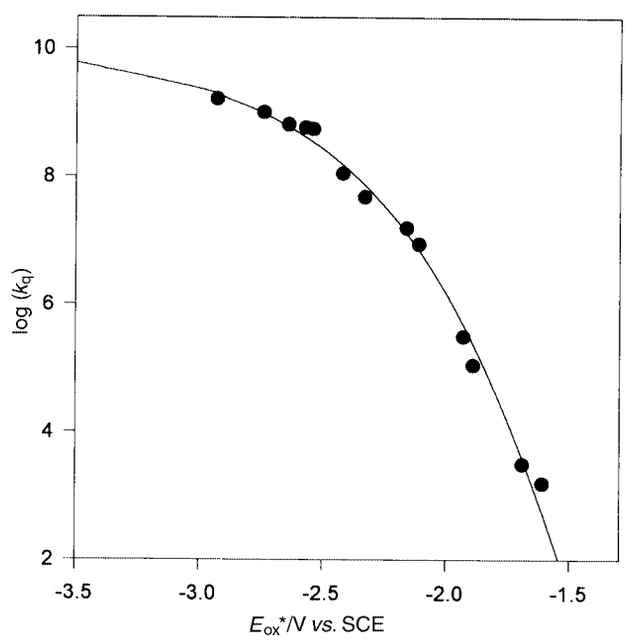

Fig. 2 Rehm–Weller analysis of the dependence of the fluorescence quenching rate constant (k_q in M^{-1} s^{-1}) for CH_2Br_2 (filled circles) on the excited state oxidation potentials (E_{ox}* in V *vs.* SCE) of various sensitizers (carbazoles and anthracenes, see Tables 5 and 7) in MeCN. Curve (solid line) shows the fit calculated according to the Rehm–Weller model.

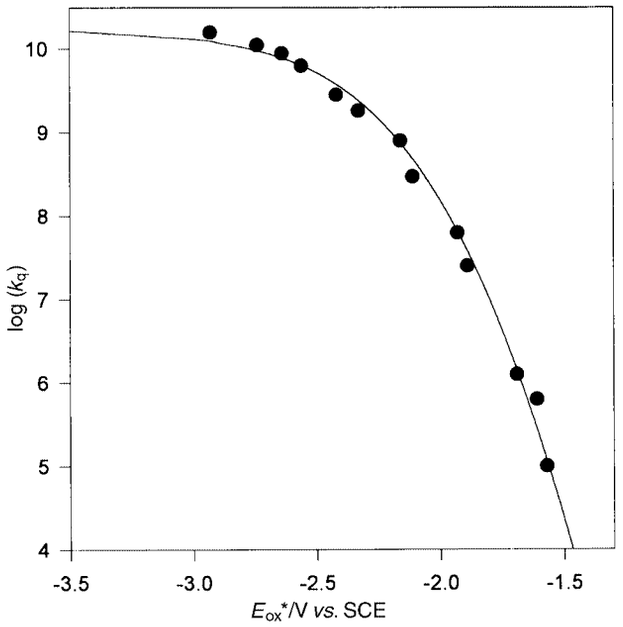

Fig. 3 Rehm–Weller analysis of the dependence of the fluorescence quenching rate constant (k_q in M^{-1} s^{-1}) for CCl_4 (filled circles) on the excited state oxidation potentials (E_{ox}* in V *vs.* SCE) of various sensitizers (carbazoles and anthracenes, see Tables 5 and 7) in MeCN. Curve (solid line) shows the fit calculated according to the Rehm–Weller model.

The uniqueness of the fits and the uncertainties in the best fit parameters were estimated by using the procedure described above for the $k_{max}K_{diff}$ parameter. This procedure was applied to the remaining parameters, λ and E_{red}. Both λ and E_{red} converged on the same best fit parameters to within the stated uncertainties. We estimated the uncertainty in λ as ±0.15 eV and the uncertainty in E_{red} as ±0.08 V.

We also fitted the data to the classical Marcus theory[44] by using our experimental k_q values. For these, eqn. (4) was replaced with eqn. (6).

$$\Delta G^{\ddagger} = (\lambda/4)(1 + \Delta G^{\circ}/\lambda)^2 \quad (6)$$

In these cases the theoretical curves did not match the experimental data as well, but similar values for E_{red} and λ were extracted from the best fits. The optimised plots from the Rehm–Weller equation (eqn. (4)) and the Marcus equation (eqn. (6)) along with the experimental data for all the quenchers used in the present study show that the former equation fits better with our experimental results.

The kinetics of the one-electron reduction potential of the halogenated compounds were analysed in the framework of the Rehm–Weller-type quadratic activation-driving force relationship starting with the assumption that the bond-breaking process, one of the possible competitive deactivation pathways of the contact ion pair, has been taken into account as part of the rate constant k_3 (Scheme 3).

From this analysis the E_{red} of the reaction step: $RX + e^- \rightarrow RX^{-\bullet}$ was estimated. In order to check the consistency of the E_{red} values obtained for the halomethanes in the present work (Table 8), we correlated these values with different thermodynamic parameters such as the electron affinity (E_A), the difference between the LUMO energy and the HOMO energy (ΔE) and the bond dissociation energy (D_{RX}). Thus, the LUMO and HOMO energy values of the halomethanes were calculated from their optimised geometries by using *ab initio* computational methods (Gaussian 98W)[30] (see "Theoretical calculations" in the Experimental section) and the energy difference, ΔE, was calculated according to eqn. (7).

$$\Delta E = E_{LUMO} - E_{HOMO} \quad (7)$$

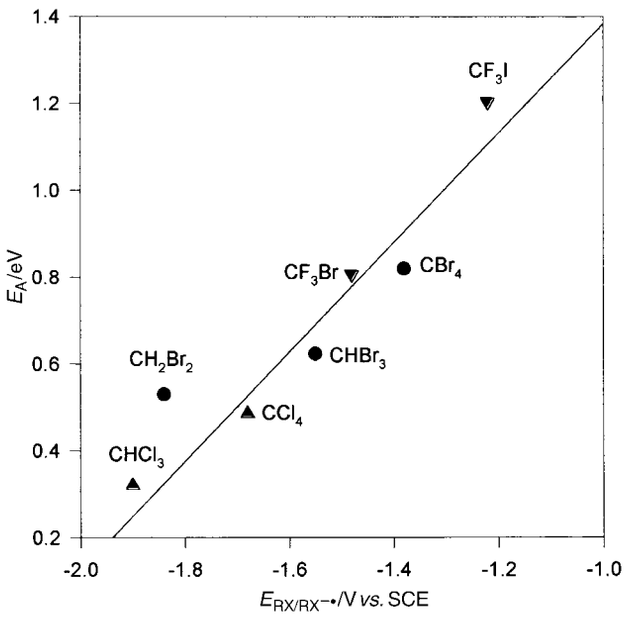

Fig. 4 Correlation between electron affinities (E_A) and one-electron reduction potentials ($E_{RX/RX^{-\bullet}}$) of the polyhalomethanes. Curve (solid line) shows the linear regression (r^2: 0.995).

Additionally, the electron affinity of the halomethanes was calculated as the difference between the heat of formation (ΔH_f) of the neutral form and the anion radical form by using *ab initio* calculation methods (see "Theoretical calculations" in the Experimental section) according to eqn. (8), where RX and

$$E_A = \Delta H_f(RX) - \Delta H_f(RX^{-\bullet}) \quad (8)$$

$RX^{-\bullet}$ represent the neutral form and the anion radical form of the halomethane RX, respectively. Finally, the bond dissociation energy (D_{RX}) values were taken from the literature.[45] In Table 6 are shown the values of the thermodynamic parameters mentioned above together with the E_{red} values of the halomethanes obtained in the present work. Also, in the same table we report the one-electron reduction potential ($E_{RX/RX^{-\bullet}}$) values for CF_3Br and CF_3I that we estimated by using the Rehm–Weller model and the electron transfer rate constant values (k_1) obtained under homogeneous catalysis by Savéant *et al.*[11]

Fig. 4 shows the E_A *vs.* $E_{RX/RX^{-\bullet}}$ plot of the halomethanes studied and a good linear regression relationship is observed. This result confirms the consistency of the one-electron reduction potential values ($E_{RX/RX^{-\bullet}}$) estimated for the halomethanes using the Rehm–Weller quadratic driving force framework. Thus, the larger the electron affinity value of the halomethane, the more oxidant capability the halomethane has towards the carbazole series.

Additionally, this linear correlation may be used to estimate the one-electron reduction potential ($E_{RX/RX^{-\bullet}}$) of polyhaloalkanes which are not easily available from cyclic voltammetric reduction of the substrate owing to its fast reduction coupled with follow-up chemical reactions of the species formed. It is worth noting that, nowadays, *ab initio* calculations offer an excellent opportunity to determine accurately absolute values of the electron affinity (E_A)[30a] to within ±0.1 eV, according to eqn. (8). As is mentioned in Table 6 (see footnote *i*), the E_A values calculated in the present work for CF_3I and CF_3Br are similar to those experimental values reported in the literature.[45d]

Simultaneously, we have improved the correlation between the one-electron reduction potential values ($E_{RX/RX^{-\bullet}}$) and the LUMO–HOMO energy difference (ΔE) of the halomethanes, respectively (see E_{red} in Table 6 and Fig. 5). The results obtained

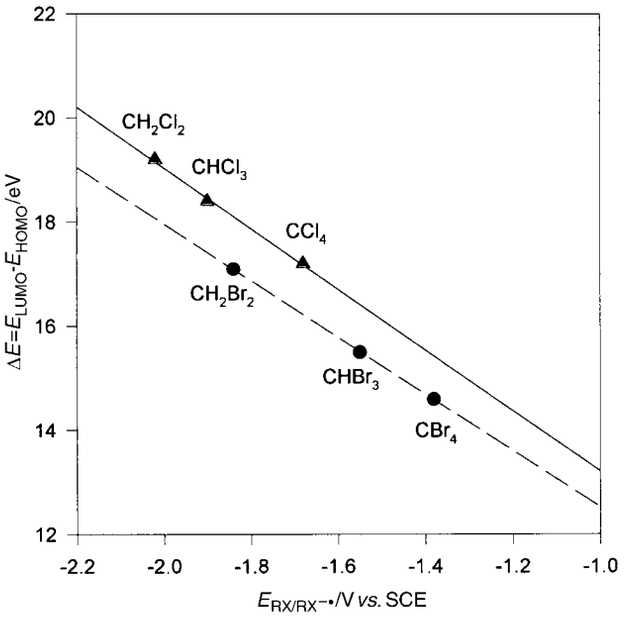

Fig. 5 Correlation between HOMO–LUMO energy difference (ΔE) and one-electron reduction potentials ($E_{RX/RX^{-\cdot}}$) of the polyhalomethanes. Solid line: linear regression of the polychloromethanes. Dashed line: linear regression of the polybromomethanes.

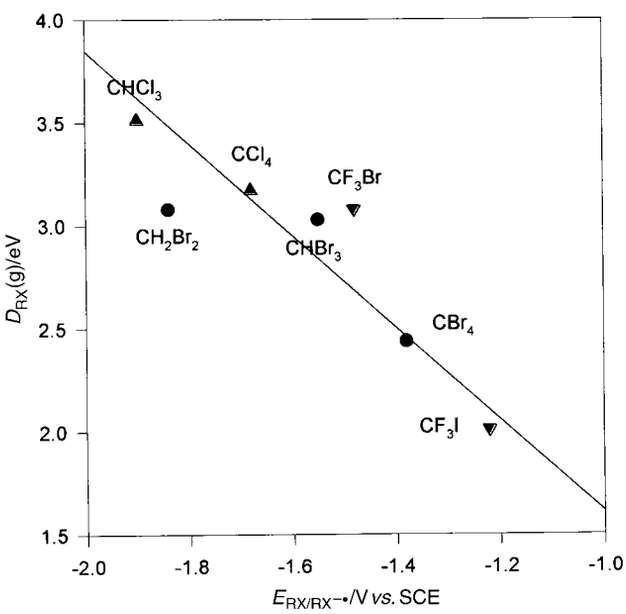

Fig. 6 Correlation between bond dissociation energies (D_{RX}) and one-electron reduction potentials ($E_{RX/RX^{-\cdot}}$) of the polyhalomethanes. Curve (solid line) shows the linear regression (r^2 : 0.990).

show a good linear correlation of the polychloro- and polybromoalkanes, but both separately as different families. This particular trend is expected due to the difference in the electronegativity of the halogen atom, *i.e.*, chloro and bromo, respectively.

Finally, we have correlated the one-electron reduction potential values ($E_{RX/RX^{-\cdot}}$) with the bond dissociation energy values (D_{RX}) of the polyhalomethanes studied in the present work (Fig. 6 and Table 6). Also, in the same figure the $E_{RX/RX^{-\cdot}}$ values of CF_3Br and CF_3I are plotted. As can be seen in Fig. 6, a good linear correlation is obtained. Taking into account that the bond dissociation energy values are available from the literature or from thermochemical cycles, this linear correlation may be also of use to estimate the $E_{RX/RX^{-\cdot}}$ values for those compounds not showing reproducible behaviour under reversible cyclic voltammetry conditions.

Another reason that supports the reaction mechanism proposed for the mathematical treatment of our experimental results is that the one-electron reduction potential of the polyhalomethanes proceeds through the intermediacy of the anion radical ($RX^{-\bullet}$) followed by a C–X bond breaking stepwise mechanism. The magnitude of the corresponding intrinsic barrier, ($\Delta G^{\ddagger}_{o}$), a thermodynamic parameter, was easily calculated from eqn. (9), where the reorganisation energy values, (λ),

$$\Delta G^{\ddagger}_{o} = \lambda/4 \quad (9)$$

are obtained from the fitting method. The $\Delta G^{\ddagger}_{o}$ values calculated are listed in Table 9. The values obtained are not very large, indicating that an outer-sphere electron transfer leading to $RX^{-\bullet}$ occurs. According to the Marcus theory,[44] λ may be represented as the sum of two factors, λ_o and λ_i (solvent reorganisation energy (λ_o) and the inner coordination sphere energy (λ_i) associated with structural changes and stretching of the carbon–halogen bond.[46]) In the present work we have calculated both parameters from independent methods. In this framework, the solvent reorganisation factor is obtained from the Marcus–Hush equation pertaining to the outer-sphere intermolecular electron transfer,[47] eqn. (10), where a is the hard-

$$\lambda_o = c[(1/a_D) + (1/a_A) - (1/d)][(1/D_{op}) - (1/D_s)] \quad (10)$$

sphere radii approximation of the donor and of the acceptor (see Table 10), d is the distance between the centres of the two equivalent spheres and D_{op} and D_s are the optical constant and relative permittivity[31] respectively. The values thus obtained are shown in Table 11. The inner coordination sphere values, λ_i, of the electron donor (carbazoles and anthracenes) and the electron acceptor (halomethanes) were calculated in this study using the PM3 method[29]–QSAR properties and *ab initio* calculation–QSAR properties respectively (see "Theoretical calculations"). The difference between ΔH_f of the radical cation with the unchanged structures from the neutral forms and ΔH_f for the optimised structures can be regarded as the rearrangement energy of the inner coordination sphere of the donor (λ_i^D) associated with the structural change upon electron transfer oxidation in the gas phase. By proceeding in the same way as described above, the inner coordination spheres of the acceptors (λ_i^A) were also determined. The λ_i^D and the λ_i^A values thus obtained are presented in Table 10, and for comparison, the experimental reorganisation energy (λ_{exp}) and the calculated reorganisation energy (λ_{calcd}) values are also shown in Table 11. The latter is the sum of the factors λ_o, λ_i^D and λ_i^A. As can be seen in Table 11, the λ_{exp} values agree with the λ_{calcd} values, showing the consistency of the outer-sphere electron transfer process leading to the halomethane anion radical ($RX^{-\bullet}$).

It is interesting to note that when a dissociative one-electron transfer process occurs as a concerted mechanism, the intrinsic barrier energy makes a contribution towards the bond breaking process. This energy is approximately equal to one-fourth of the dissociation energy of the bond to be broken.[45,48,49] This model was recently developed by Savéant[48] for monohalogenated aliphatic compounds, to calculate the intrinsic barrier ($\Delta G^{\ddagger}_{o}$) using eqn. (11), where the D_{RX} value is the R–X bond dissociation energy of the halomethane in the gas phase.[45a] Taking into account the model, we calculated values of $\Delta G^{\ddagger}_{o}$, which are listed in Table 9. For comparison, the $\Delta G^{\ddagger}_{o}$ values experimentally measured and the theoretical $\Delta G^{\ddagger}_{o}$ values calculated as the sum of the factors λ_o, λ_i^A and λ_i^D are shown in the same table. As can be seen in Table 9 the magnitudes of the former $\Delta G^{\ddagger}_{o}$ values (eqn. (11)) are larger than those obtained

$$\Delta G^{\ddagger}_{o} = (D_{RX} + \lambda_o + \lambda_i)/4 \quad (11)$$

experimentally. In previous reports,[12a–d,37] Ekstrom and Eberson claim that the λ values calculated for CBr_4 and CCl_4 are 98 kcal

mol^{-1} (4.2 eV) and 120 kcal mol^{-1} (5.2 eV) respectively. These λ values were estimated by using the k values measured for the product formation, including the one-electron transfer process and the C–X bond breaking process (C–Br and C–Cl, respectively). Thus, we conclude that the photoinduced one-electron reduction of the halomethanes is more likely to proceed *via* a stepwise electron transfer process through the intermediacy of the $RX^{-\bullet}$ anion radical than a concerted electron transfer–bond breaking mechanism.

Another fundamental thermodynamic parameter to be determined is the free enthalpy of the homolytic dissociation of the C–X bond in the anion radicals. For this, we need to know the dissociative one-electron reduction potential of the halomethanes ($E_{RX/R^{\bullet}+X^-}$). To the best of our knowledge, these values are not available in the literature, thus we needed to estimate the standard potential $E_{RX/R^{\bullet}+X^-}$ *versus* the aqueous saturated calomel electrode in each solvent,[50] using eqn. (12) (where the potentials are expressed in volts and the free energies in eV; *i.e.*, RX: CCl_4, $R^{\bullet}$: $Cl_3C^{\bullet}$, X^-: Cl^-).

$$E_{RX/R^{\bullet}+X^-} = \Delta E^{o,solvent}(SHE \rightarrow SCE) + G^{f,solvent}(RX) - G^{f,solvent}(R^{\bullet}) - G^{f,solvent}(X^-) = \Delta E^{o,solvent}(SHE \rightarrow SCE) + G^{f,gas}(RX) - G^{f,gas}(R^{\bullet}) - G^{f,solvent}(X^-) + \Delta G^{\circ}(RX/R^{\bullet}) \quad (12)$$

$\Delta E^{o,solvent}(SHE \rightarrow SCE)$ is the potential shift when passing from the standard hydrogen electrode in the solvent to the aqueous SCE. The values are equal to −0.255 V for both MeCN and EtOH. $G^{f,gas}(RX)$ and $G^{f,gas}(R^{\bullet})$ are the Gibbs free energies of formation of RX and $R^{\bullet}$ in the gas phase. Their values are equal to −0.12 (CH_2Br_2), −1.2 ($CHCl_3$), −0.97 (CCl_4), 0.48 ($CHBr_3$), 1.80 ($BrCH_2^{\bullet}$), 1.05 ($Cl_2CH^{\bullet}$), 0.82 ($Cl_3C^{\bullet}$) and 2.35 ($Br_2CH^{\bullet}$) eV.[45b]

The Gibbs free energies of formation of CBr_4 and $CBr_3^{\bullet}$ in the gas phase were calculated using *ab initio* methods. Their values are equal to 1.43 (CBr_4) and 2.78 ($Br_3C^{\bullet}$) eV. The Gibbs free energy of the halide ion formation in a particular solvent, $G^{f,solvent}(X^-)$ is equal to −0.923 (Cl^-) and −0.784 (Br^-) eV in MeCN[51] and to −1.230 (Cl^-) and −0.961 (Br^-) eV in EtOH.[51] There are two ways to solve the problem of estimating the standard Gibbs free energy $\Delta G^{\circ}_{RX/R^{\bullet}}$ of reaction (13). One is

$$RX\ (solvent) + R^{\bullet}\ (gas) \rightarrow RX\ (gas) + R^{\bullet}\ (solvent) \quad (13)$$

simply to neglect it. The other is to assume that (i) for methyl halide its value is the same in the solvents used (acetonitrile and ethanol) and in water, and (ii) that the Gibbs free energy of CH_3 from the gas phase to water is the same as that of CH_4. Taking into account the above assumptions, the $\Delta G^{\circ}_{RX/R^{\bullet}}$ values obtained are 0.112 and 0.121 eV for chloro- and bromomethanes,[52] respectively. The ensuing values of $E_{RX/R^{\bullet}+X^-}$ are listed in Table 12.

Once the one-electron reduction potential is known, the next step is to estimate the free enthalpy of the C–X homolytic dissociation of the anion radical of the halomethanes. Taking into account that a stepwise process occurs,[11] this value can be calculated from eqn. (14), where the $\Delta G^{f,solvent}$ values are the free

$$E_{RX/RX^{-\bullet}} = \Delta G^{f,solvent}(RX) - \Delta G^{f,solvent}(RX^{-\bullet}) \quad (14)$$

enthalpies of formation of the species RX and $RX^{-\bullet}$ in the solvent. Thus, we obtain eqn. (15), where the latter term is the standard free enthalpy of C–X bond dissociation of the halomethane anion radical in the solvent. The $E_{RX/RX^{-\bullet}}$ values were determined in this study and the $E_{RX/R^{\bullet}+X^-}$ values were estimated as we discussed above. Thus, the $\Delta G^{o,diss}$ values were easily calculated from eqn. (15) and they are shown in Table 13.

$$E_{RX/RX^{-\bullet}} = E_{RX/R^{\bullet}+X^-} + \Delta G^{o,diss}(RX^{-\bullet}) \quad (15)$$

As can be seen the free enthalpy of dissociation of the anion radical has a largely negative value which indicates that the halomethane anion radical is quite unstable in the reaction medium (acetonitrile and ethanol). Thus, it can be concluded that once the halomethane anion radical is formed, it decomposes in the solvent cage into the halomethyl radical and the halide anion. However, we consider that the electron transfer process occurs preferentially as a stepwise rather than a concerted carbon–halogen bond breaking process because our results include the finding of low-to-moderate quantum efficiencies for the photochemical yields of chlorocarbazoles.[22]

When the photochemical reaction of carbazole and *N*-acetylcarbazole is carried out in the presence of CCl_4 under degassed conditions, the quantum efficiencies of substrate conversion (ϕ) are substantially lower than unity (Table 4). These values were obtained under conditions in which quenching of carbazole excited singlet states is nearly complete. These results indicate that the halide radical anions must survive long enough within the initial ion pair formed in the quenching step to be able to undergo considerable back-electron transfer (Scheme 3). The quantum yield values lower than unity for the degassed samples are attributed to the competition between fragmentation of the acceptor anion radical and the return electron transfer process. It should be noted that Klassen and Ross[53] have observed the transient absorption spectrum of $CCl_4^{-\bullet}$ (λ_{max}: 370 nm) in 3-methylpentane at 95 K. At this temperature, this species decays over 1 ms. At room temperature, this decay will be greatly enhanced, but, in our experiments, it may only be necessary for $CCl_4^{-\bullet}$ to live for tens of picoseconds in order to participate in the back-electron transfer process with its geminate radical cation partner. Recently, in agreement with our results, Robert and Savéant have reported, from first principles, that a purely dissociative photoinduced electron transfer is not necessarily endowed with a unity quantum yield.[54] Additionally, these results confirm that the back-electron transfer step is an important reaction pathway and that it competes with the other deactivation process of the contact ion pair to give the carbazoles and the quenchers in the ground state (Scheme 3). This means that the anion radicals of the halomethanes have a fleeting existence, although we were not able to detect these species.

Conclusions

In the present study we were able to determine the reorganisation energy (λ) of the photoinduced electron transfer reduction of a variety of polyhalomethanes by a series of carbazoles and anthracenes in terms of the quenching rate constants (k_q) in acetonitrile and in ethanol solution by using the Rehm–Weller Gibbs energy relationship. The λ values thus obtained were compared with the solvent reorganisation energy (λ_o) and the calculated inner sphere coordination energy (λ_i) and a good correlation was observed. The magnitude of the average free enthalpy energy at zero driving force ($\Delta G^{\ddagger}_o$), calculated from the relation $\Delta G^{\ddagger}_o = \lambda/4$, was not too large so an outer-sphere electron transfer leading to the contact ion radical pair is proposed.

We also determined the one-electron reduction potential ($E_{RX/RX^{-\bullet}}$) of a variety of polyhalogenated methanes by using the same quadratic driving force and relating it to the concerted one-electron transfer–bond breaking reduction potential, where the standard free enthalpy of dissociation of $RX^{-\bullet}$ was estimated.

The one-electron reduction potential values ($E_{RX/RX^{-\bullet}}$) estimated in acetonitrile were correlated to different thermodynamic parameters such as electron affinity (E_A) and the LUMO–HOMO energy difference (ΔE), both calculated by *ab initio* methods, and the bond dissociation energy (D_{RX}). In all these cases good linear correlations were observed. These results showed the consistency of the estimated $E_{RX/RX^{-\bullet}}$ values

obtained in the present work by using the Rehm–Weller Gibbs energy relationship. Since the electron affinities (E_A) of the polyhalomethanes studied in this work satisfactorily correlate to the estimated $E_{RX/RX^{-\cdot}}$ values, this kind of linear correlation may be used to estimate the $E_{RX/RX^{-\cdot}}$ values of other polyhalogenated compounds and electron acceptors in general, which are not directly available from cyclic voltammetry measurements.

Taking into account the quantum yield values of substrate disappearance obtained from the preparative photochemical irradiations, which are lower than unity, we concluded that the photoinduced electron transfer reduction of the halomethanes occurs stepwise through the intermediacy of the anion radical and the homolytic dissociation step of this transient competes significantly with the back-electron transfer process.

Acknowledgements

The authors thank Universidad de Buenos Aires (TW34) and CONICET PIP 0904 (Resol.2851/98) for partial financial support; Dr H. Nonami (Ehime University, Japan) for some chemicals, HyperChem Suite (Prof.) 5.1 program and computational facilities; Dr F. Quina (Federal University of San Pablo, Brazil) for use of an Edinburgh OB900 fluorometer and his generous hospitality; Dr G. Burton (DQO, FCEyN, UBA) for Gaussian 98W and Lic. E. M. Sproviero (DQO, FCEyN, UBA) for useful discussions about *ab initio* calculations. R. Erra-Balsells is a research member of CONICET.

References

1 For recent reviews, see, for example; (*a*) A. Albini and A. Sulpizio, in *Photoinduced electron transfer*, M. A. Fox and M. Chanon, Eds., Elsevier, Amsterdam, 1988, Part C, p. 88; (*b*) J. K. Kochi, *Acta Chem. Scand.*, 1990, **44**, 409; (*c*) F. D. Saeva, *Top. Curr. Chem.*, 1990, **156**, 59.
2 P. Maslak, J. Kula and J. E. Chateauneuf, *J. Am. Chem. Soc.*, 1991, **13**, 2304.
3 J. D. Simon and K. S. Peter, *Organometallics*, 1991, **2**, 1876.
4 M. Ohashi, S. Otami and S. Kyushin, *Chem. Lett.*, 1991, 631.
5 M. Mautner, P. Neta, R. K. Norris and K. J. Wilson, *J. Phys. Chem.*, 1986, **90**, 168.
6 P. Neta and D. Behar, *J. Am. Chem. Soc.*, 1981, **103**, 103.
7 (*a*) C. P. Andrieux, A. Le Gorande and J. M. Savéant, *J. Am. Chem. Soc.*, 1992, **114**, 6892; (*b*) J. M. Savéant, *J. Am. Chem. Soc.*, 1992, **114**, 10595.
8 (*a*) J. M. Savéant, *Acc. Chem. Res.*, 1993, **26**, 455; (*b*) J. M. Savéant, *Dissociative Electron Transfer*, in *Advances in Electron Transfer Chemistry*, P. S. Mariano, Ed., JAI Press, New York, 1994, vol. 4, pp. 53–116; (*c*) C. P. Andrieux, J. M. Savéant and C. Tardy, *J. Am. Chem. Soc.*, 1997, **119**, 11546 and references cited therein.
9 I. Chen, M. S. Farahat, E. R. Gaillard, S. Farid and D. G. Whitten, *J. Photochem. Photobiol. A*: *Chem.*, 1996, **95**, 21.
10 B. R. Arnold, J. C. Scaiano and W. G. McGimpsey, *J. Am. Chem. Soc.*, 1992, **114**, 9978.
11 C. P. Andrieux, L. Gelis, M. Medebielle, J. Pinson and J. M. Savéant, *J. Am. Chem. Soc.*, 1990, **112**, 3509.
12 (*a*) L. Eberson and M. Ekstrom, *Acta Chem. Scand.*, *Sect. B*, 1988, **41**, 40; (*b*) L. Eberson and M. Ekstrom, *Acta Chem. Scand.*, *Sect. B*, 1988, **42**, 101; (*c*) L. Eberson and M. Ekstrom, *Acta Chem. Scand.*, *Sect. B*, 1988, **42**, 113; (*d*) L. Eberson, M. Ekstrom, T. Lund and H. Lund, *Acta Chem. Scand.*, *Sect. B*, 1989, **43**, 101.
13 M. von Stackelberg and W. Z. Strack, *Elektrochem.*, 1949, **53**, 118; J. Casanova and L. Eberson, *The Chemistry of the carbon halogen bond*, S. Patai, Ed., Wiley, New York, 1973, p. 979.
14 S. P. Mishra and M. C. R. Symons, *J. Chem. Soc.*, *Chem. Commun.*, 1973, 577; E. Kh. Brickenstein and R. F. Khairutdinov, *Chem. Phys. Lett.*, 1982, **115**, 176.
15 C. P. Andrieux, J. M. Savéant and C. Tardy, *J. Am. Chem. Soc.*, 1998, **120**, 4167.
16 E. R. Gaillard and D. G. Whitten, *Acc. Chem. Res.*, 1996, **29**, 292.
17 S. L. Mattes and S. Farid, *Acc. Chem. Res.*, 1982, **15**, 80.
18 J. P. Dinnocenzo, W. P. Todd, T. R. Simpson and I. R. Gould, *J. Am. Chem. Soc.*, 1990, **112**, 2468.
19 V. C. Yoon, P. S. Mariano, R. S. Givens and B. W. Atwater, in *Advances in Electron Transfer in Chemistry*, Ed. P. S. Mariano, JAI Press, Greenwich CT, 1994, vol. 4.
20 D. G. Whitten, C. Chesta, X. Ci, M. A. Kellett and V. W. Yan, in *Photochemical Processes in Organized Molecular Systems*, K. Honda, Ed., Elsevier, Amsterdam, 1991.
21 P. Maslak, Jr., W. H. Chapman, Jr., T. M. Vallombroso and B. A. Watson, *Can. J. Chem.*, 1975, **53**, 3175.
22 (*a*) S. M. Bonesi and R. Erra-Balsells, *J. Photochem. Photobiol. A*: *Chem.*, 1997, **110**, 271; (*b*) S. M. Bonesi, PhD Thesis, Universidad de Buenos Aires, 1995.
23 S. M. Bonesi and R. Erra-Balsells, *J. Photochem. Photobiol. A*: *Chem.*, 1991, **56**, 55.
24 (*a*) S. M. Bonesi and R. Erra-Balsells, *J. Heterocycl. Chem.*, 1991, **28**, 1035; (*b*) S. M. Bonesi and R. Erra-Balsells, *An. Asoc. Quim. Argent.*, 1991, **79**, 113.
25 S. M. Bonesi and R. Erra-Balsells, *J. Heterocycl. Chem.*, 1997, **34**, 877.
26 S. M. Bonesi and R. Erra-Balsells, *J. Heterocycl. Chem.*, 1997, **34**, 891.
27 D. D. Perrin and W. L. F. Armarego, *Purification of Laboratory Chemicals*, 3rd edn., Pergamon Press, New York, 1988.
28 C. G. Hatchard and C. A. Parker, *Proc. R. Soc. London, Ser. A*, 1956, **235**, 518.
29 (*a*) HyperChem Suite, Autodesk Inc., Ontario, 1998; (*b*) T. A. Clark, *Handbook of Computational Chemistry*, Wiley, New York, 1985, p. 97; (*c*) A. D. Becke, *Phys. Rev. A*, 1988, **38**, 3098; (*d*) C. Lee, W. Yang and R. G. Parr, *Phys. Rev. B*, 1988, **37**, 785; (*e*) A. D. Becke, *J. Chem. Phys.*, 1993, **98**, 5648.
30 (*a*) J. B. Foresman and A. E. Frisch, *Exploring Chemistry with Electronic Structure*, Gaussian Inc., Pittsburgh, 1996; (*b*) Gaussian 98, Revision A.3, M. J. Frisch, G. W. Trucks, H. B. Schlegel, E. G. Scuseria, M. A. Robb, J. R. Cheeseman, V. G. Zakrzewski, J. A. Montgomery, Jr., R. E. Stratmann, J. C. Burant, S. Dapprich, J. M. Millam, A. D. Daniels, K. N. Kudin, M. C. Strain, O. Farkas, J. Tomasi, V. Barone, M. Cossi, R. Cammi, B. Mennucci, C. Pomelli, B. Adamo, S. Clifford, J. Ochterski, G. A. Petersson, P. Y. Ayala, Q. Cui, K. Morokuma, D. K. Malick, A. D. Rabuck, K. Raghavachari, J. B. Foresman, J. Cioslowski, J. V. Ortiz, B. B. Stefanov, G. Liu, A. Liashenko, P. Piskorz, I. Komaromi, R. Gomperts, R. L. Martin, D. J. Fox, T. Keith, L. A. Al-Laham, C. Y. Peng, A. Nanayakkara, C. Gonzalez, M. Challacombe, P. M. W. Gill, B. Johnson, W. Chen, M. W. Wong, J. L. Andres, C. Gonzalez, M. Head-Gordon, E. S. Replogle, J. A. Pople, Gaussian, Inc., Pittsburgh PA, 1998.
31 S. L. Murov, I. Carmicheal and G. L. Hug, *Handbook of Photochemistry*, 2nd edn., Marcel Dekker Inc., New York, 1993.
32 G. J. Kavarnos and N. J. Turro, *J. Chem. Rev.*, 1986, **86**, 401.
33 (*a*) J. Ambrose and R. F. Nelson, *J. Electrochem. Soc.*, 1968, **115**, 1159; (*b*) L. L. Carpenter and R. F. Nelson, *J. Electrochem. Soc.*, 1975, **122**, 876; (*c*) B. Reitstoen and V. D. Parker, *J. Am. Chem. Soc.*, 1991, **113**, 6954.
34 M. Chanon, M. D. Hawley and M. A. Fox, *Photoinduced Electron Transfer*, M. Chanon, M. A. Fox, Eds., Elsevier, Amsterdam, 1988, Part A, p. 1.
35 P. S. Mariano and J. L. Stavinoha, in *Synthetic Organic Photochemistry*, W. M. Horspool, Ed., Plenum Press, New York, 1984, pp. 145–257.
36 (*a*) A. Rehm and A. Weller, *Ber. Bunsenges. Phys. Chem.*, 1969, **73**, 839; (*b*) A. Rehm and A. Weller, *Isr. J. Chem.*, 1970, **8**, 259.
37 L. Eberson, *Electron Transfer Reactions in Organic Chemistry*, Springer Verlag, Berlin, Germany, 1987.
38 J. P. Soumillon, *Top. Curr. Chem.*, 1993, **168**, 93.
39 S. T. Murphy, C. Zon, J. B. Miers, R. M. Ballew, D. D. Dlott and G. B. Schuster, *J. Phys. Chem.*, 1993, **97**, 13252.
40 S. Murphy and G. B. Schuster, *J. Phys. Chem.*, 1995, **99**, 511.
41 B. Legros, P. Vandereencken and J. P. Soumillion, *J. Phys. Chem.*, 1991, **95**, 4752.
42 R. A. Marcus, *Int. J. Chem. Kinet.*, 1981, **13**, 865.
43 G. E. McManis, M. N. Golovin and M. J. Weaver, *J. Phys. Chem.*, 1986, **90**, 6563.
44 R. A. Marcus, *J. Chem. Phys.*, 1956, **24**, 4966.
45 (*a*) *Handbook of Chemistry and Physics*, 66th edn., CRC, Cleveland, OH, 1985, p. F185; (*b*) *Handbook of Chemistry and Physics*, 66th edn., CRC, Cleveland, OH, 1985, p. F191; (*c*) *Handbook of Chemistry and Physics*, 75th edn., CRC, Cleveland, OH, 1995, Table 3, pp. 9–66; (*d*) *Handbook of Chemistry and Physics*, 75th edn., CRC, Cleveland, OH, 1995, Table 4, pp. 10–185.
46 A. Hasegawa, M. Shiotani and F. William, *Faraday Discuss. Chem. Soc.*, 1977, 157.
47 (*a*) N. S. Hush, *J. Chem. Phys.*, 1958, **28**, 967; (*b*) R. A. Marcus, in *Theory and Application of electron transfer at Electrodes and in*

solution, *Special topics in electrochemistry*, P. A. Rock, Ed., Elsevier, New York, 1977, pp. 161–179.
48 J. M. Savéant, *J. Am. Chem. Soc.*, 1978, **109**, 6788.
49 J. M. Savéant, *Adv. Phys. Org. Chem.*, 1990, **26**,1.
50 J. M. Savéant, *J. Am. Chem. Soc.*, 1987, **109**, 6788 and references cited therein.
51 (*a*) B. G. Cox, G. R. Hedvig, A. J. Parker and D. W. Watts, *Aust. J. Chem.*, 1974, **27**, 477; (*b*) D. H. Geske, M. A. Ragle, J. L. Bambeneck and A. L. Blach, *J. Am. Chem. Soc.*, 1964, **86**, 987; (*c*) *Handbook of Chemistry and Physics*, 66th edn., CRC, Cleveland, OH, 1985, p. D50.
52 (*a*) N. S. Z. Hush, *Electrochemistry*, 1957, **61**, 734; (*b*) L. Eberson, *Acta Chem. Scand.*, *Sect. B*, 1982, **36**, 533.
53 N. V. Klassen and C. K. Ross, *J. Phys. Chem.*, 1987, **91**, 3668.
54 M. Robert and J. M. Savéant, *J. Am. Chem. Soc.*, 2000, **122**, 514.